Visual Neuroscience (2015), **32**, e018, 6 pages.

doi:10.1017/S0952523815000139

BRIEF COMMUNICATION

Rod- and cone-isolated flicker electroretinograms and their response summation characteristics

J. JASON MCANANY,[1,2,3,*] JASON C. PARK,[1] AND DINGCAI CAO[1]

[1]Department of Ophthalmology and Visual Sciences, University of Illinois at Chicago, Chicago, Illinois 60612
[2]Department of Psychology, University of Illinois at Chicago, Chicago, Illinois 60612
[3]Department of Bioengineering, University of Illinois at Chicago, Chicago, Illinois 60607

(RECEIVED February 24, 2015; ACCEPTED April 21, 2015)

Abstract

This study defined the amplitude and phase characteristics of rod- and cone-isolated flicker electroretinograms (ERGs) and determined how these responses summate to generate the nonreceptor-specific ERG. Full-field ERGs were obtained from six normally sighted subjects (age 26 to 44 years) using a four-primary LED-based photostimulator and standard recording techniques. The four primaries were either modulated sinusoidally in phase to achieve simultaneous rod and cone activation (ERG_{R+C}; nonreceptor-specific) or in different phases to achieve rod-isolated (ERG_R) and cone-isolated (ERG_C) responses by means of triple silent substitution. ERGs were measured at two mean luminance levels (2.4 and 24 cd/m^2), two contrasts (20 and 40%), and four temporal frequencies (2–15 Hz). Fundamental amplitude and phase for each condition were derived by Fourier analysis. Response amplitude and phase depended on the stimulus conditions (frequency, mean luminance, and contrast), however, for all conditions: 1) response phase decreased monotonically as stimulus frequency increased; 2) response amplitude tended to decrease monotonically as stimulus frequency increased, with the exception of the 24 cd/m^2, 40% contrast ERG_{R+C} that was sharply V-shaped; 3) ERG_R phase was delayed (32 to 210 deg) relative to the ERG_C phase; 4) ERG_R amplitude was typically equal to or lower than the ERG_C amplitude, with the exception of the 2.4 cd/m^2, 40% contrast condition; and 5) the pattern of ERG_{R+C} responses could be accounted for by a vector summation model of the rod and cone pathway signals. The results show that the ERG_{R+C} amplitude and phase can be predicted from ERG_R and ERG_C amplitude and phase. For conditions that elicit ERG_R and ERG_C responses that have approximately equal amplitude and opposite phase, there is strong destructive interference between the rod and cone responses that attenuates the ERG_{R+C}. Conditions that elicit equal amplitude and opposite phase rod and cone responses may be particularly useful for evaluating rod–cone interactions.

Keywords: Electroretinogram (ERG), Rod, Cone, Flicker

Introduction

The full-field electroretinogram (ERG) is a measure of the electrical response of the retina to light stimulation and is recorded clinically to evaluate the functional integrity of the rod and cone pathways. A standard paradigm has been established by the International Society for Clinical Electrophysiology of Vision (ISCEV) that recommends recording ERGs for different adaptation conditions (light- and dark-adapted) and different stimulus parameters to target the rod and cone pathways independently (McCulloch et al., 2015). For example, ERGs mediated by the rod pathway are measured using a brief, low-luminance pulse following a period of dark adaptation, whereas ERGs mediated by the cone pathway are measured with a brief, high-luminance pulse (and 30 Hz flicker) following light adaptation. There are also conditions under which the ERG is generated by a combination of both rod and cone pathway responses. For example, the ISCEV standard brief, high-luminance flash delivered to the dark-adapted eye elicits a response from both the rod and cone pathways, the so-called "mixed response."

The studies describing the nature in which the rod and cone ERG responses combine (e.g., Cao et al., 2011) and the transition from a rod-dominated response to a cone-dominated response due to increasing adaptation level (Bijveld et al., 2011*a*; Bijveld et al., 2011*b*; Nagy et al., 2014; Park et al., 2015) have recently been reported. Cao et al. (2011) isolated rod- and cone-generated ERGs based on the principle of silent substitution (Estevez & Spekreijse, 1982) and compared rod- and cone-isolated ERGs to those obtained when both rod and cone activities were modulated simultaneously. With the silent substitution approach, the quantal catch of one receptor class (e.g., the rod photoreceptors) is constant during the stimulus presentation, whereas the quantal catch of the other receptor class (e.g., short-, medium-, and long-wavelength sensitive cones) is modulated systematically. The excitation of each receptor class can be calculated based on the spectral radiance of the stimulus and

*Address correspondence to: J. Jason McAnany, Department of Ophthalmology and Visual Sciences, University of Illinois at Chicago, 1855 W. Taylor St., Chicago, IL 60612. E-mail: jmcana1@uic.edu

the receptor fundamentals (Shapiro et al., 1996). When combined with sinusoidally modulated stimuli, the silent substitution approach is particularly powerful because ERG amplitude and phase information can be obtained for rod- and cone-isolated responses under conditions in which the time-averaged luminance, chromaticity, and state of adaptation are constant. Moreover, this permits interactions between the rod- and cone-pathway-driven ERGs to be evaluated by comparing the receptor-isolated responses to nonreceptor-specific responses.

Previous ERG results (Kremers & Scholl, 2001; Cao et al., 2011; Park et al., 2015) as well as psychophysical results (MacLeod, 1972; van den Berg & Spekreijse, 1977) have shown that the combination of rod- and cone-pathway signals can be described quantitatively by vector summation. Vector summation models make a strong prediction regarding the ERG generated by combined rod and cone responses (i.e., the nonreceptor-specific ERG): under conditions in which the rod- and cone-isolated ERGs have equal amplitude and opposite phase (i.e., 180 deg phase difference), the nonreceptor-specific ERG will be abolished. Identifying the stimulus luminance and temporal frequency characteristics that elicit equal amplitude and opposite phase rod- and cone-generated ERGs would provide a useful tool for studying rod–cone interactions and would also be a clear test of the vector summation model. Previous ERG studies that have examined rod–cone interactions have done so under conditions of relatively low luminance, where the cone-isolated response is small (Cao et al., 2011), or under conditions of relatively high luminance, where the rod-isolated response is small (Kremers & Scholl, 2001; Kremers & Pangeni, 2012). Thus, rod-isolated, cone-isolated, and nonreceptor-specific ERGs have not been studied systematically using temporal frequency, contrast, and adaptation conditions that elicit similar amplitude rod- and cone-isolated ERGs.

The purpose of this study was to define the amplitude and phase characteristics of rod- and cone-isolated flicker ERGs and to determine how rod and cone responses summate to generate the nonreceptor-specific flicker ERG. A four-primary photostimulator was implemented to generate three types of temporally modulated stimuli based on the principle of silent substitution: 1) rod-isolating stimuli in which cone excitation was kept constant (ERG_R), 2) cone-isolating stimuli in which S-, M-, and L-cone excitations were modulated in phase while keeping the rod excitation constant (ERG_C), 3) combined rod- and cone-modulating stimuli in which both rod and cone excitations were modulated in phase (ERG_{R+C}). ERG_{R+C} amplitude and phase were predicted using a vector summation model (Kremers & Scholl, 2001; Cao et al., 2011) based on the amplitudes and phases of the ERG_R and ERG_C responses measured at different stimulus mean luminance levels, contrasts, and temporal frequencies.

Materials and methods

Subjects

Six subjects (five male and one female; age 26 to 44 years) with no history of eye disease, normal color vision (Oculus Heidelberg Multi-Color Anomaloscope), and ETDRS best-corrected visual acuity of 0 log MAR or better (equivalent to 20/20 or better Snellen acuity) participated in the study. Informed consent was obtained from all the subjects before their participation. Procedures adhered to the tenets of the Declaration of Helsinki, and the protocol was approved by an Institutional Review Board at the University of Illinois at Chicago.

Apparatus and stimuli

The apparatus is described elsewhere (McAnany & Nolan, 2014; Park et al., 2015). In brief, full-field stimuli were generated by a Diagnosys Espion E^3 system and presented in a ColorDome desktop ganzfeld (Diagnosys LLC, Lowell, MA). Stimuli were the sum of four LED-generated light sources [dominant wavelengths of 465 nm (blue), 515 nm(green), 593 nm (amber), and 642 nm (red)]. The four LEDs were simultaneously modulated sinusoidally in phase to achieve combined rod and cone modulation or in different phases to achieve rod or cone isolation, as defined elsewhere (Cao et al., 2011; Park et al., 2015). The chromaticity was constant under all three paradigms (CIE 10° coordinates of $x = 0.58$ and $y = 0.40$). ERGs were recorded at two mean luminance levels (2.4 and 24 scot. cd/m^2) and four different stimulus temporal frequencies (2, 4, 8, and 15 Hz). In the primary experiment, ERGs were obtained from the six subjects using rod, cone, and combined rod- and cone-modulating stimuli that had a Michelson contrast of 40%. Of note, 40% contrast was the maximum achievable contrast under the cone-isolating paradigm, so the contrast was set to 40% under all three paradigms. In a follow-up experiment performed in a subset of the subjects ($N = 4$), the contrast of the rod-isolating stimulus was reduced to 20%. Similarly, the rod contrast of the combined rod- and cone-modulating stimulus was also reduced to 20%. Stimulus wavelength and luminance were measured using a Spectrascan 740 spectroradiometer (Photo Research, Chatsworth, CA).

The degree of rod and cone isolation is a potential concern in silent substitution paradigms. However, a recent study from our group (Park et al., 2015) that used identical 15 Hz rod-modulating, cone-modulating, and combined rod- and cone-modulating stimuli and instrumentation found good isolation, based on the results obtained from a patient with achromatopsia. Specifically, the 15 Hz flicker ERG_{R+C} and ERG_R responses obtained from this patient, who lacked a cone response, were highly similar to each other and to the ERG_R responses obtained from visually normal subjects, indicating negligible cone intrusion under the ERG_R paradigm. Furthermore, an earlier study from our group that used similar stimuli and instrumentation showed that the impact of isolation error, principally due to lens transmittance, is minimal in subjects younger than 45 years (Cao et al., 2011).

Procedure and ERG recording

Prior to the monocular ERG recordings, the pupil of the tested eye was dilated with 1% tropicamide and 2.5% phenylephrine hydrochloride drops, and the fellow eye was patched. The subject was dark adapted for 30 min. ERGs were recorded with DTL plus fiber electrodes; ear clip and gold cup (forehead) electrodes served as reference and ground, respectively. Responses were acquired with an Espion E^3 electrophysiology console, with amplifier bandpass settings of 0.30–500 Hz at a sampling frequency of 1 kHz.

ERG recordings for the primary experiment were conducted in a single session lasting approximately 90 min. The follow-up experiment at 20% contrast was performed in a second session that lasted approximately 60 min. For each temporal frequency at each luminance level, 5–10 ERG sweeps were recorded. Each sweep was approximately 5 s in duration (the exact duration of the sweep depended on the stimulus period), with an even number of cycles. The stimulus modulation was followed by a dark interval (minimum of 7 s) before the next sweep began. The subject was alerted to minimize eye blinks and movements by a short tone at

http://dx.doi.org/10.1017/S0952523815000139

the beginning of each sweep. Cycles contaminated by eye movement and blink artifacts were removed off-line during the data analysis procedure.

Data analysis

The initial 2–16 cycles, depending on stimulus frequency, were omitted from the analysis to avoid onset transients (approximately 1 s). The remaining 8–60 cycles (approximately 4 s) of each sweep were divided into an even number of segments and these segments were averaged. This procedure was repeated for each of the 5–10 sweeps obtained for each stimulus to generate an overall average. Fast Fourier transforms (FFTs) were performed on the overall average to derive the amplitude and phase of the fundamental component. In the figures below, the phases are given in cosine phase and are "unwrapped" to extend beyond 360°, per convention. A subject's response at a given stimulus luminance was considered distinguishable from noise if the amplitude at the stimulus frequency was at least 2.82 times larger than the mean of the noise amplitudes measured at neighboring frequencies (±1 Hz above and below the stimulus frequency). As discussed elsewhere (Meigen & Bach, 1999), a signal-to-noise ratio (SNR) of 2.82 corresponds to a significance level of $P = 0.05$. Individual responses that did not achieve an SNR of at least 2.82 were excluded from the mean results presented below.

Results

ERG_R, ERG_C, and ERG_{R+C} 40% contrast stimuli: Effect of mean luminance

Fig. 1 shows the mean (±1 SEM) log fundamental amplitude (left column) and phase (right column) as a function of log stimulus temporal frequency for the six subjects under the rod-isolating (top row), cone-isolating (middle row), and the nonreceptor-specific (bottom row) paradigms. Linear equivalents of the log frequencies are given on the top *x*-axes. Data were obtained at 40% contrast at mean luminance levels of 2.4 and 24 cd/m^2, represented by the open and filled symbols, respectively. At 2.4 cd/m^2, the ERG_R amplitude function was low-pass in shape on log–log axes, decreasing as temporal frequency increased. A similar pattern was observed at 24 cd/m^2. In general, the primary effect of increasing mean luminance from 2.4 to 24 cd/m^2 was to shift the ERG_R function downward. The ERG_R phase functions were highly similar at the two luminance levels, both decreasing monotonically as temporal frequency increased.

The shape of the ERG_C amplitude functions (middle row) differed from the ERG_R amplitude functions. That is, log ERG_C amplitude decreased approximately linearly as log temporal frequency increased from 2 to 8 Hz for both mean luminance levels. The amplitude functions obtained at the two luminance levels diverged slightly at 15 Hz, where the ERG_C amplitude measured at 2.4 cd/m^2 continued to decrease and the amplitude at 24 cd/m^2 increased. The ERG_C phase functions decreased monotonically as temporal frequency increased. The ERG_C phases were similar for the two lowest frequencies and diverged for the two highest frequencies, with the response at 2.4 cd/m^2 having a slight lag (60 deg) compared to the response obtained at 24 cd/m^2.

The shape of the ERG_{R+C} amplitude functions (bottom row) obtained at 2.4 and 24 cd/m^2 differed substantially, unlike the

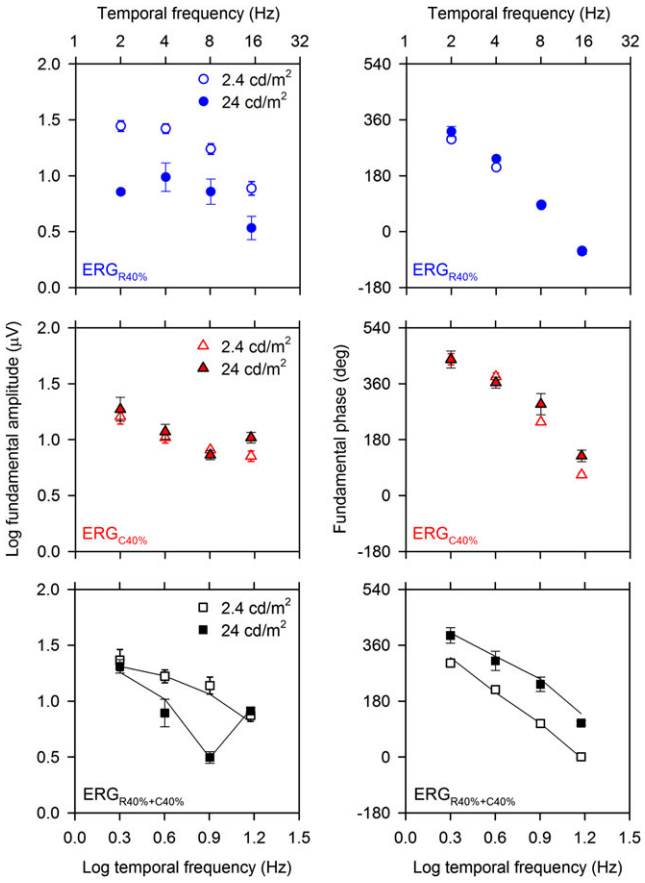

Fig. 1. Mean (±1 SEM) log fundamental amplitude (first column) and phase (second column) as a function of log stimulus temporal frequency. Data were obtained with a stimulus contrast of 40%. Data are shown for two luminance levels (open symbols, 2.4 cd/m^2; filled symbols 24 cd/m^2) for the rod-isolating condition (top row), cone-isolating condition (middle row), and nonreceptor-specific condition (bottom row). The solid lines fit to the nonreceptor-specific data represent the results of a vector summation model, as described in the text.

ERG_R and ERG_C amplitude functions that were generally similar at the two luminance levels. At 2.4 cd/m^2, ERG_{R+C} log amplitude decreased monotonically with log temporal frequency, whereas at 24 cd/m^2, log amplitude decreased sharply from 2 to 8 Hz, then increased sharply from 8 to 15 Hz. The phase functions obtained at the two luminance levels were similar in shape but were shifted by approximately 90° from each other. The solid lines represent the results of a vector summation model fit to the data, as described elsewhere (Cao et al., 2011). In brief, ERG_{R+C} can be estimated by summing the amplitudes of the ERG_R and ERG_C responses, taking into account the ERG_R and ERG_C phases. The vector summation model prediction for the ERG_{R+C} data was performed separately for each mean luminance level, each temporal frequency, and each subject. The model provided a good description of the amplitude and phase data at high luminance (mean R^2 was >0.93 for both amplitude and phase averaged across temporal frequency and subject) and low luminance (mean R^2 was >0.81 for both amplitude and phase averaged across temporal frequency and subject). Good fits of the model to the data were also reported in previous studies (Kremers & Scholl, 2001; Cao et al., 2011; Park et al., 2015), providing further support that the rod and cone responses combine vectorially to yield the ERG_{R+C}.

http://dx.doi.org/10.1017/S0952523815000139

ERG_R, ERG_C, and ERG_{R+C} 40% contrast stimuli: Effect of paradigm

The data of Fig. 1 are replotted in Fig. 2 to allow direct comparisons of the effects of stimulus temporal frequency on ERG_R, ERG_C, and ERG_{R+C} amplitude (left column) and phase (right column). Data obtained at 2.4 and 24 cd/m^2 are shown in the first and second rows, respectively. At 2.4 cd/m^2, the ERG_R amplitude was larger than ERG_C and ERG_{R+C} amplitudes, except at 15 Hz where the amplitudes obtained under the three conditions were similar (upper left panel). The phases of the ERG_R and ERG_{R+C} at 2.4 cd/m^2 were similar and shifted by 142 to 176 deg from the ERG_C function from 2 to 8 Hz; at 15 Hz, the ERG_R and ERG_{R+C} phases differed slightly (59 deg) and were shifted from the ERG_C phase (upper right panel). The approximately counter-phase ERG_R and ERG_C responses observed from 2 to 8 Hz produce destructive interference, which accounts for why the ERG_{R+C} amplitude was smaller than the ERG_R amplitude across this range.

At 24 cd/m^2 (Fig. 2, bottom row), ERG_R and ERG_C amplitudes were similar at 4 and 8 Hz and differed at 2 and 15 Hz, with the ERG_R amplitude being smaller than the ERG_C amplitude. The ERG_{R+C} amplitude was similar to the ERG_C amplitude, with the exception of the response obtained at 8 Hz, where the ERG_{R+C} amplitude was smaller than the ERG_C amplitude. The ERG_R and ERG_C phases differed substantially at all temporal frequencies (116 to 210 deg), with the largest differences occurring at 8 and 15 Hz (lower right panel). The ERG_{R+C} phase was generally similar to the ERG_C phase but was shifted by approximately 50 deg from 2 to 8 Hz. At 8 Hz, the ERG_R and ERG_C amplitudes were nearly equal and the phases differed by 210 deg, which resulted in strong attenuation of the ERG_{R+C} response and accounts for the sharp notch at 8 Hz in the ERG_{R+C} amplitude function. Although the ERG_R and ERG_C responses were also approximately counter-phase at 15 Hz (192 deg phase difference), the ERG_R amplitude was substantially smaller than the ERG_C amplitude, which resulted in minimal destructive interference at this frequency.

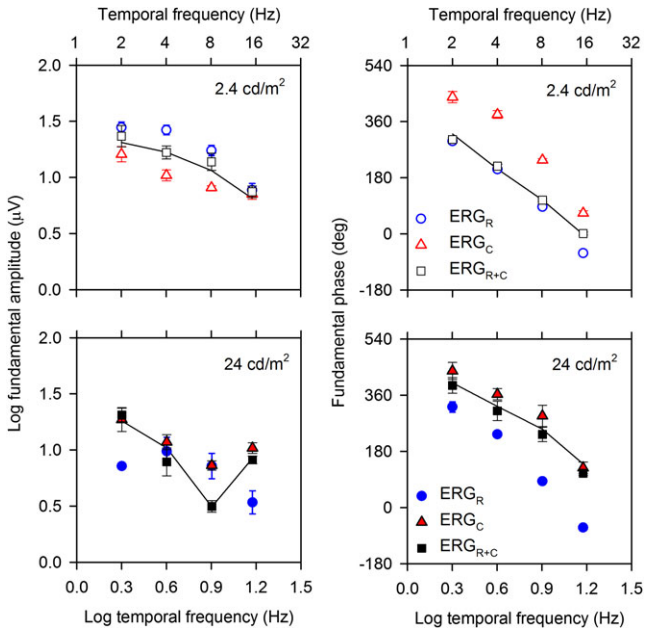

Fig. 2. Mean (±1 SEM) log fundamental amplitude (first column) and phase (second column) as a function of log stimulus temporal frequency. Data were obtained with a stimulus contrast of 40%. Data are shown for mean luminance levels of 2.4 cd/m^2 (top row) and 24 cd/m^2 (bottom row). Data from the rod-isolating condition (circles), cone-isolating condition (triangles), and nonreceptor-specific condition (squares) are shown.

ERG_R and ERG_{R+C}: Effect of contrast

The results of Figs. 1 and 2 suggest that with appropriate selection of stimulus mean luminance level and flicker frequency, the conditions can be identified that elicit ERG_R and ERG_C responses of approximately equal amplitude and opposite phase. Under these conditions, the amplitude of the ERG_{R+C} is strongly attenuated. As an alternative means of producing rod- and cone-pathway ERGs of approximately equal amplitude and opposite phase, the contrast of the rod-isolating stimulus was reduced by half (from 40 to 20%). The amplitude of the ERG elicited by the low contrast rod stimulus ($ERG_{R20\%}$) is expected to be reduced compared to that of the 40% rod-isolating stimulus, producing a vertical downward shift in the 40% contrast ERG_R functions shown in Fig. 2. Two predicted outcomes of reducing the rod-pathway response are as follows: 1) at 2.4 cd/m^2, a downward shift of the 40% contrast ERG_R function may result in amplitudes that more closely match the 40% contrast ERG_C amplitude, generating increased destructive interference that alters the shape of the nonreceptor-specific function; 2) at 24 cd/m^2, a downward shift of the 40% contrast ERG_R function may result in amplitudes that differ substantially from the 40% contrast ERG_C amplitudes, generating minimal destructive interference for the nonreceptor-specific condition. These predictions can be evaluated in Fig. 3, which shows response amplitude (left column) and phase (right column) for responses obtained at mean luminance levels of 2.4 (top row) and 24 cd/m^2 (bottom row). The circles represent the response amplitude and phase obtained for rod-isolating stimuli that had 20% contrast ($ERG_{R20\%}$); the red triangles represent the response to cone-isolating stimuli that had 40% contrast ($ERG_{C40\%}$); the black squares show the response amplitude and phase obtained for a stimulus that had 20% rod contrast and 40% cone contrast ($ERG_{R20\%+C40\%}$). The gray lines are the vector summation model predictions for the 40% contrast ERG_{R+C} (for the four subjects who participated in the reduced contrast experiment).

At 2.4 cd/m^2 (top row), reducing the contrast of the rod-isolating stimulus from 40 to 20% ($ERG_{R20\%}$; blue circles) reduced the rod-isolated response amplitude by approximately 0.45 log units. Importantly, at 4 and 8 Hz, the $ERG_{R20\%}$ amplitude was similar to the $ERG_{C40\%}$ amplitude (red triangles), but the phases of these responses were nearly opposite (152 deg difference at 4 Hz and 149 deg difference at 8 Hz). The shape of the $ERG_{R20\%+C40\%}$ amplitude function (weakly V-shaped) was different from the 40% contrast ERG_{R+C} amplitude function (low-pass; gray line). The shape change can be explained by interactions between rod and cone pathway responses that are relatively strong for the $ERG_{R20\%+C40\%}$, compared to the 40% contrast ERG_{R+C}. The shapes of the $ERG_{R20\%+C40\%}$ phase function (black line) and the 40% contrast ERG_{R+C} function (gray line) were similar, but the 40% contrast phase function was lagged (approximately 40–100 deg, depending on stimulus temporal frequency).

At 24 cd/m^2 (bottom row), reducing the contrast of the rod-isolating stimulus from 40 to 20% ($ERG_{R20\%}$; blue circles) reduced the amplitude by approximately 0.45 log units, but the shift was somewhat less uniform compared to that at 2.4 cd/m^2. The $ERG_{R20\%}$ amplitude was substantially smaller than the $ERG_{C40\%}$ amplitude at all temporal frequencies. Consequently, there was minimal rod–cone interaction in the $ERG_{R20\%+C40\%}$ response, despite the nearly

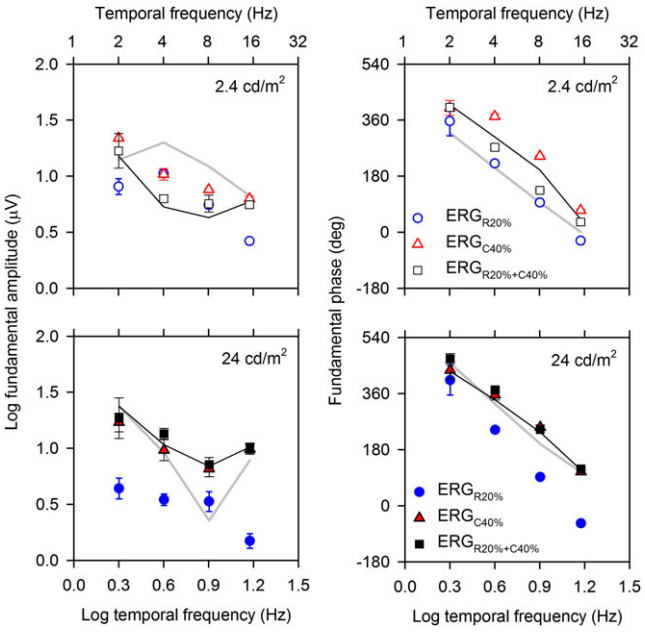

Fig. 3. Mean (±1 SEM) log fundamental amplitude (first column) and phase (second column) as a function of log stimulus temporal frequency. Data are shown for mean luminance levels of 2.4 cd/m^2 (top row) and 24 cd/m^2 (bottom row). Data from the 20% contrast rod-isolating condition (circles), 40% contrast cone-isolating condition (triangles), and nonreceptor-specific condition (20% rod contrast, 40% cone contrast; squares) are shown. The gray lines represent the 40% ERG_{R+C} vector summation model fits and are shown to facilitate comparison with the $ERG_{R20\%+C40\%}$.

opposite phases at 8 and 15 Hz for the $ERG_{R20\%}$ and $ERG_{C40\%}$ (approximately 160 deg phase difference). Thus, the $ERG_{R20\%+C40\%}$ was cone-pathway dominated at 24 cd/m^2 because of the minimal rod response, as evidenced by the superimposition of the $ERG_{R20\%+C40\%}$ and $ERG_{C40\%}$ responses. The $ERG_{R20\%+C40\%}$ amplitude was similar to that of the 40% contrast ERG_{R+C} amplitude, with the exception of the response measured at 8 Hz, which was strongly attenuated for the 40% contrast stimulus (gray line) but not for the 20% contrast stimulus. The phase functions obtained with the 40% contrast (gray line) and 20% contrast (black line) were highly similar, indicating minimal effect of contrast on response phase for the 24 cd/m^2 ERG_{R+C} stimuli.

The vector summation model prediction applied to the data in Figs. 1 and 2 was also used to predict the $ERG_{R20\%+C40\%}$ responses in Fig. 3 (solid black lines). The vector summation model prediction for $ERG_{R20\%+C40\%}$ was performed separately for each mean luminance level, temporal frequency, and subject. This model provided a good description of the amplitude and phase data at both high luminance (mean R^2 averaged across temporal frequency and subject of 0.65 and 0.67 for amplitude and phase, respectively) and low luminance (mean R^2 averaged across temporal frequency and subject of 0.78 and 0.99 for amplitude and phase, respectively). Thus, the vector summation model accounted well for the nonreceptor-specific responses for all temporal frequencies, mean luminances, and contrasts tested.

Discussion

The purpose of this study was to define the amplitude and phase characteristics of rod- and cone-isolated flicker ERGs and to determine how rod and cone responses summate to generate the nonreceptor-specific flicker ERG. The results of the present study indicate that measuring rod-isolating, cone-isolating, and nonreceptor-specific ERGs at approximately 8 Hz, using 40% contrast sine wave flicker having a mean luminance of approximately 24 cd/m^2 may be useful for studying rod–cone interactions in the human ERG. That is, with this combination of temporal frequency, contrast, and adaptation level, there is strong destructive interference from signals arising from the rod and cone pathways that result in marked attenuation of the nonreceptor-specific ERG amplitude. However, it is likely that the combination of temporal frequency, adaptation level, and contrast that generated strong destructive interference in the present study is only one of multiple such combinations that would generate robust rod–cone interactions. Nevertheless, the stimulus characteristics identified in the present study that generated strong rod–cone interactions in our visually normal subjects may be useful in future studies and may have application to patient populations as well.

The present study focused on the fundamental response component derived by FFT (i.e., the response component corresponding to the stimulus frequency). However, nonlinear response components are often present in the flicker ERG and these harmonics have been used as an indicator of cone pathway contributions to the ERG. For example, using 15 Hz flicker stimuli presented to the dark-adapted eye, Bijveld et al. (2011*b*) showed negligible second harmonic response components for low-luminance stimuli (less than approximately –0.5 log scot. td s, presumably rod-mediated), whereas the second harmonic increased sharply as stimulus luminance increased (>1 log scot. td s, presumably cone-mediated), suggesting that the higher harmonics originated from the cone pathway. Consistent with this finding, they also showed that a patient with achromatopsia lacked the second harmonic response at all luminance levels. In the present study, the second harmonic response components generally did not exceed the noise level (SNR < 2.82). There were a few conditions at both luminance levels in which individual subjects had harmonic responses with SNR > 2.82, but the amplitudes were small and the phases varied substantially among the subjects, suggesting that the responses were largely noise-mediated. The absence of significant second harmonic response components for the cone-isolated ERG and for the nonreceptor-specific ERG in the present study is likely due to the relatively low contrast and mean luminance levels used.

Multiple types of rod–cone interaction have been reported (MacLeod, 1972; Alexander & Fishman, 1984; Coletta & Adams, 1984; Lange et al., 1997; Cao et al., 2006; Zele & Cao, 2014), but the present study focused on the direct interaction of signals generated by the rod and cone pathways. Although the site of the rod–cone interaction assessed by the ERG is presently uncertain, a vector summation model of rod- and cone-driven responses provided an excellent account of the data, consistent with previous ERG studies (Kremers & Scholl, 2001; Cao et al., 2011; Park et al., 2015). The ability of the vector summation model to account for the nonreceptor-specific response is also consistent with physiological experiments showing that rod and cone signals are combined in a vector sum fashion in retinal ganglion cells (Cao et al., 2010) and in lateral geniculate nucleus cells of the magnocellular and the parvocellular pathways (Lee et al., 1997; Weiss et al., 1998).

In summary, rod- and cone-isolated ERGs can be obtained based on the principle of silent substitution. By manipulating the stimulus temporal frequency, adaptation level, and contrast, rod- and cone-isolated ERGs can be recorded that have approximately equal amplitude and opposite phase. The nonreceptor-specific ERG is

reduced in amplitude when recorded under these conditions. The reduced nonreceptor-specific ERG amplitude is due to destructive interference between the rod and cone pathway responses, which can be accounted for by a vector summation model. Stimuli that generate rod and cone pathway responses of equal amplitude and opposite phase may be particularly useful in future studies for evaluating rod–cone interactions, given the strong destructive interference for the nonreceptor-specific ERG under these conditions.

Acknowledgments

This research was supported by National Institutes of Health Research Grants R00EY019510 (JM), P30EY001792 (departmental core grant), and an unrestricted departmental grant from Research to Prevent Blindness.

References

Alexander, K.R. & Fishman, G.A. (1984). Rod-cone interaction in flicker perimetry. *The British Journal of Ophthalmology* **68**, 303–309.

Bijveld, M.M., Kappers, A.M., Riemslag, F.C., Hoeben, F.P., Vrijling, A.C. & van Genderen, M.M. (2011a). An extended 15 Hz ERG protocol (1): The contributions of primary and secondary rod pathways and the cone pathway. *Documenta Ophthalmologica* **123**, 149–159.

Bijveld, M.M., Riemslag, F.C., Kappers, A.M., Hoeben, F.P. & van Genderen, M.M. (2011b). An extended 15 Hz ERG protocol (2): Data of normal subjects and patients with achromatopsia, CSNB1, and CSNB2. *Documenta Ophthalmologica* **123**, 161–172.

Cao, D., Lee, B.B. & Sun, H. (2010). Combination of rod and cone inputs in parasol ganglion cells of the magnocellular pathway. *Journal of Vision* **10**, 4.

Cao, D., Pokorny, J. & Grassi, M.A. (2011). Isolated mesopic rod and cone electroretinograms realized with a four-primary method. *Documenta Ophthalmologica* **123**, 29–41.

Cao, D., Zele, A.J. & Pokorny, J. (2006). Dark-adapted rod suppression of cone flicker detection: Evaluation of receptoral and postreceptoral interactions. *Visual Neuroscience* **23**, 531–537.

Coletta, N.J. & Adams, A.J. (1984). Rod-cone interaction in flicker detection. *Vision Research* **24**, 1333–1340.

Estevez, O. & Spekreijse, H. (1982). The "silent substitution" method in visual research. *Vision Research* **22**, 681–691.

Kremers, J. & Pangeni, G. (2012). Electroretinographic responses to photoreceptor specific sine wave modulation. *Journal of the Optical Society of America. A, Optics, Image Science, and Vision* **29**, A306–A313.

Kremers, J. & Scholl, H.P. (2001). Rod-/L-cone and rod-/M-cone interactions in electroretinograms at different temporal frequencies. *Visual Neuroscience* **18**, 339–351.

Lange, G., Denny, N. & Frumkes, T.E. (1997). Suppressive rod-cone interactions: Evidence for separate retinal (temporal) and extraretinal (spatial) mechanisms in achromatic vision. *Journal of the Optical Society of America. A, Optics, Image Science, and Vision* **14**, 2487–2498.

Lee, B.B., Smith, V.C., Pokorny, J. & Kremers, J. (1997). Rod inputs to macaque ganglion cells. *Vision Research* **37**, 2813–2828.

MacLeod, D.I. (1972). Rods cancel cones in flicker. *Nature* **235**, 173–174.

McAnany, J.J. & Nolan, P.R. (2014). Changes in the harmonic components of the flicker electroretinogram during light adaptation. *Documenta Ophthalmologica* **129**, 1–8.

McCulloch, D.L., Marmor, M.F., Brigell, M.G., Hamilton, R., Holder, G.E., Tzekov, R. & Bach, M. (2015). ISCEV Standard for full-field clinical electroretinography (2015 update). *Documenta Ophthalmologica* **130**, 1–12.

Meigen, T. & Bach, M. (1999). On the statistical significance of electrophysiological steady-state responses. *Documenta Ophthalmologica* **98**, 207–232.

Nagy, B.V., Barboni, M.T., Martins, C.M., da Costa, M.F., Kremers, J. & Ventura, D.F. (2014). Human flicker electroretinography using different temporal modulations at mesopic and photopic luminance levels. *Documenta Ophthalmologica* **129**, 129–138.

Park, J.C., Cao, D., Collison, F.T., Fishman, G.A. & McAnany, J.J. (2015). Rod and cone contributions to the dark-adapted 15-Hz flicker electroretinogram. *Documenta Ophthalmologica* **130**, 111–119.

Shapiro, A.G., Pokorny, J. & Smith, V.C. (1996). Cone-rod receptor spaces with illustrations that use CRT phosphor and light-emitting-diode spectra. *Journal of the Optical Society of America. A, Optics, Image Science, and Vision* **13**, 2319–2328.

van den Berg, T.J. & Spekreijse, H. (1977). Interaction between rod and cone signals studied with temporal sine wave stimulation. *Journal of the Optical Society of America* **67**, 1210–1217.

Weiss, S., Kremers, J. & Maurer, J. (1998). Interaction between rod and cone signals in responses of lateral geniculate neurons in dichromatic marmosets (*Callithrix jacchus*). *Visual Neuroscience* **15**, 931–943.

Zele, A.J. & Cao, D. (2014). Vision under mesopic and scotopic illumination. *Frontiers in Psychology* **5**, 1594.